Langmuir Decay Instability Cascade in Laser-Plasma Experiments

S. Depierreux,[1,*] C. Labaune,[1] J. Fuchs,[1] D. Pesme,[2] V. T. Tikhonchuk,[3] and H. A. Baldis[4]

[1]*Laboratoire pour l'Utilisation des Lasers Intenses, UMR No. 7605 CNRS-École Polytechnique-CEA-Université Paris VI, École Polytechnique, 91128 Palaiseau Cedex, France*

[2]*Centre de Physique Théorique, UMR No. 7644 CNRS-École Polytechnique, 91128 Palaiseau Cedex, France*

[3]*Institut de Physique Fondamentale, Université Bordeaux-1, 33405 Talence Cedex, France*

[4]*Institute for Laser Science and Applications, Lawrence Livermore National Laboratory, P.O. Box 808, Livermore, California 94550*

(Received 3 August 2001; published 8 July 2002)

Thomson scattering has been used to investigate the nonlinear evolution of electron plasma waves (EPWs) generated by stimulated Raman scattering (SRS). Two complementary diagnostics demonstrate the occurrence of the cascade of Langmuir decay instabilities (LDI). The EPW wave-number spectrum displays an asymmetric broadening towards small wave numbers, interpreted as a signature of the secondary EPWs produced in the LDI cascade. The number of cascade steps is in agreement with the broadening of the associated ion-acoustic-waves' spectra. The total energy transferred in the EPWs cascade is found to be either less than or of the same order of magnitude as the energy of the primary EPW.

DOI: 10.1103/PhysRevLett.89.045001 PACS numbers: 52.38.Bv, 52.35.Fp, 52.35.Mw, 52.70.Kz

The control of laser-plasma instabilities represents an important component of the laser-driven inertial confinement fusion (ICF) research. The future megajoule lasers [1,2] will give rise to plasma conditions for which these instabilities might grow at a level so high that the linear description fails. Their final excitation level will consequently be determined by saturation mechanisms [3] whose identification and comprehension are prerequisite for an efficient control. In this Letter, we present new experimental results concerning the nonlinear evolution of the stimulated Raman scattering (SRS). SRS is the parametric instability by which the incident laser wave decays into an electron plasma wave (EPW) and another transverse wave. It could be detrimental in ICF experiments because the scattered light decreases the laser/plasma coupling [4] and may affect the irradiation symmetry. In addition, the EPWs accelerate electrons which may preheat the fusion fuel.

A possible saturation mechanism for this instability is the coupling of the SRS-generated EPW (henceforth named the primary EPW, and denoted as EPW1) to the ion acoustic waves (IAW). Depending on the value of the quantity $k_{\mathrm{EPW1}}\lambda_{\mathrm{De}}$ (here k_{EPW1} denotes the EPW1 wave number and λ_{De} is the Debye length), this coupling may give rise to (i) the Langmuir decay instability (LDI) [5] in the regime $k_{\mathrm{EPW1}}\lambda_{\mathrm{De}} > 0.2$ [LDI is the process by which the primary EPW decays into a secondary EPW (EPW2) and an ion acoustic wave (IAW2); this process may repeat itself, the secondary EPW2 decaying into another EPW (EPW3) and IAW (IAW3), thus generating the so-called LDI cascade] and (ii) the Langmuir collapse [6,7] in the opposite regime $k_{\mathrm{EPW1}}\lambda_{\mathrm{De}} < 0.2$. The EPW1 wave number in our experiment lies in the domain $k_{\mathrm{EPW1}}\lambda_{\mathrm{De}} \sim 0.2-0.3$, so that the coupling of the primary EPW to the IAWs could give rise to the LDI cascade. The LDI cascade may be viewed as corresponding to an energy sink for the primary EPW, because the secondary EPWs are nonresonant for SRS. Therefore, the LDI cascade can be expected to be an efficient nonlinear saturation mechanism for SRS.

The LDI occurrence has been demonstrated in a previous experiment [8] where the two decay products, namely the secondary IAW and EPW, were observed simultaneously. The Thomson scattering (TS) spectra of IAWs exhibited two components interpreted as the evidence of the first LDI cascade step. Counterpropagating IAWs (see Fig. 1a) produced by the initial LDI of the primary EPW and by the first step in the LDI cascade were respectively probed by down and up TS giving two peaks in the IAW spectrum separated by 3.5 Å. The next steps in the LDI cascade could not be resolved, because the large Doppler effect in the expanding plasma broadened each peak by 0.5 Å, whereas the separation between the peaks corresponding to the IAWs produced in successive even cascade steps (IAW2 and IAW4) was 0.2 Å only [9].

In the present experiment, we set up a new diagnostic to k-resolve the EPW spectra for a well-defined electron density in order to eliminate the strong dependence of k_{EPW1} on the time evolving density. Above a laser threshold of 2×10^{13} W/cm^2, the k spectra show an asymmetric broadening towards small wave numbers, consistently with the LDI cascade. This broadening is interpreted as due to the contribution of the EPWs produced in the LDI cascade, up to the seventh secondary EPW. Because the decay products are all probed with a unique TS geometry, the k spectra give an accurate measurement of their relative intensity. These observations are of fundamental importance in the context of SRS saturation because the EPW and IAW evolutions determine the energy balance in the SRS process.

Four beams of the Laboratoire pour l'Utilisation des Lasers Intenses (LULI) facility (see Fig. 1b) were used to

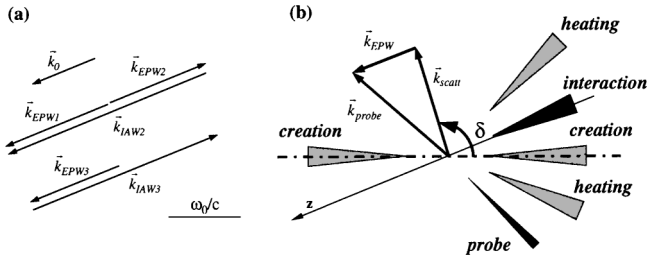

FIG. 1. (a) Wave-vector diagram for the Langmuir cascade of SRS-driven EPWs. This diagram is for $n_e/n_c = 0.1$, where n_c is the critical density at 1 μm. $\vec{k}_0$ is the incident laser wave vector, $\vec{k}_{\mathrm{EPW1}}$ is the EPW wave vector stimulated by Raman backscattering, $\vec{k}_{\mathrm{EPW}n}$ and $\vec{k}_{\mathrm{IAW}n}$ are the wave vectors of the EPWs and IAWs produced in step n of the LDI cascade. Their moduli are $|\vec{k}_{\mathrm{EPW}n}| = |\vec{k}_{\mathrm{EPW1}}| - (n-1)\Delta k$ and $|\vec{k}_{\mathrm{IAW}n}| = 2|\vec{k}_{\mathrm{EPW1}}| - (2n-3)\Delta k$ with $\Delta k = (2/3\lambda_{\mathrm{De}})\sqrt{Zm_e/m_i}$, where λ_{De} is the Debye length. (b) Experimental setup and wave-vector diagram for down-TS off an EPW. This latter satisfies $\vec{k}_{\mathrm{scatt}} = \vec{k}_{\mathrm{probe}} - \vec{k}_{\mathrm{EPW}}$ and $\omega_{\mathrm{scatt}} = \omega_{\mathrm{probe}} - \omega_{\mathrm{EPW}}$, where $\vec{k}_{\mathrm{probe}}(\omega_{\mathrm{probe}})$, $\vec{k}_{\mathrm{scatt}}(\omega_{\mathrm{scatt}})$, and $\vec{k}_{\mathrm{EPW}}(\omega_{\mathrm{EPW}})$ are, respectively, the probe, scattered light, and EPW wave vectors (angular frequencies).

create and preheat a well-characterized underdense plasma which then interacts with a fifth beam at fundamental wavelength (1.053 μm, ω_0) smoothed by a random phase plate [10] and focused by an $F/6$ lens with a resulting peak intensity of 10^{14} W/cm^2. The last beam, synchronized with the interaction beam, was used as a $3\omega_0$ TS probe, the scattered light being collected by an off-axis parabolic mirror. The SRS EPWs and the EPWs produced in the successive odd LDI cascade steps were probed by down-TS, whose geometry is shown in Fig. 1b. For the measured electron temperature of 0.7 keV, the probed EPW wave vector is uniquely determined by the electron density (n_e/n_c) and by the directions of probe and scattered lights. In order to maximize the TS diagnostic resolution, we used in our experiment aperture masks so that the aperture of the probe beam was only 1°, leaving only two free parameters for the TS geometry: (i) the electron density, n_e/n_c, and (ii) the scattered light direction, δ (see Fig. 1b). The direction of the probe beam (63° with respect to the interaction beam) was chosen to match the down-scattering geometry for probing the primary EPWs produced by SRS in the backward direction within 5°, as well as the EPWs generated in the odd cascade steps. The scattered light was analyzed by a diagnostic setup combining a spectrometer, a cylindrical lens, and a camera, yielding direct measurements of the scattered light angle, δ, and wavelength, λ_{scatt} [11]. The electron density was known from the frequency matching condition $n_e/n_c = (3 - \lambda_0/\lambda_{\mathrm{scatt}})^2\,(1 + 3k_{\mathrm{EPW}}^2\lambda_{\mathrm{De}}^2)^{-1}$, and the EPW wave number could be accurately deduced from the measurement of the scattered light angle δ.

Typical spectra recorded with this diagnostic for different incident laser energies are shown in Fig. 2. The collection volume was located in the front part of the plasma at 250 μm from the initial target plane where we observed the maximum of Raman activity [8]. The strong dependence of the scattered angle on the scattered wavelength is due to the dependence of k_{EPW1} on the electron density. To account for the variation of the density during the measurements, we have indicated in Fig. 2 (the tilted stray lines) the ω-k relation for the primary SRS-driven EPW. It can be seen that for all spectra the brightest signal is along this line, demonstrating that EPW1 corresponds to a plasma wave satisfying the linear dispersion relation in the electron density decreasing with time. In the case of low laser energy (17 J), the (ω, k) spectrum shown in Fig. 2a includes two signals around $\lambda_{\mathrm{scatt}} = 3880$ and 3960 Å, with $\delta = 108°$ and 111°, respectively. All the scattered light signal falls very close to the EPW1 line, demonstrating that in the low laser energy case the scattering is due to the EPW1 only.

By contrast, in the case of higher laser intensities (Figs. 2b and 2c), a large broadening towards smaller wave vectors is observed in addition to the EPW1 signal. The broadening is the largest at the wavelength corresponding to the peak of the SRS activity. This one shifts towards larger densities when the laser energy is increased. The black curve in Fig. 3a represents, for the spectrum of Fig. 2b recorded with a laser energy of 24 J, the scattered intensity integrated over 40 Å around $\lambda_{\mathrm{scatt}} = 3820$ Å ($n_e/n_c = 0.055$) for which the broadening is maximum, as a function of the probed EPW wave vector. The signal has a maximum at $k_{\mathrm{EPW}} = 1.7\omega_0/c$, which is exactly the expected value of k_{EPW1} for $n_e/n_c = 0.055$. The observed broadening can be seen as the contribution of the EPWs produced in the successive odd LDI cascade steps. Each LDI step contribution is inferred by decomposing the measured signal as the sum of successive EPW peaks whose positions along the wave-vector axis are known from the LDI resonance conditions. The shape of each peak is given by the instrumental width resulting from the finite probe beam aperture and by density integration due to the finite wavelength resolution. The corresponding experimental width of 3° ($\delta k = 0.14\omega_0/c$) is of the same order as the expected separation between the EPW1 and EPW3 peaks, explaining why we do not observe separated peaks. The relative intensities of the peaks are uniquely determined, step by step, by a best fit between the measured signal and the decomposition into the sum of cascade peaks. The result is shown by the gray curves in Fig. 3a. Seven LDI cascade steps are needed to reproduce the measured broadening. The relative intensity ratio between the cascade components 1:3:5:7 is measured to be 1:0.55:0.35:0.2. Assuming that the even cascades satisfy a similar relation, the total energy transferred in the cascade EPWs is approximately 2 times larger than the energy of the primary EPW.

In the high laser energy case of 68 J, Fig. 2c, the scattered intensity is 100 times larger than in the intermediate

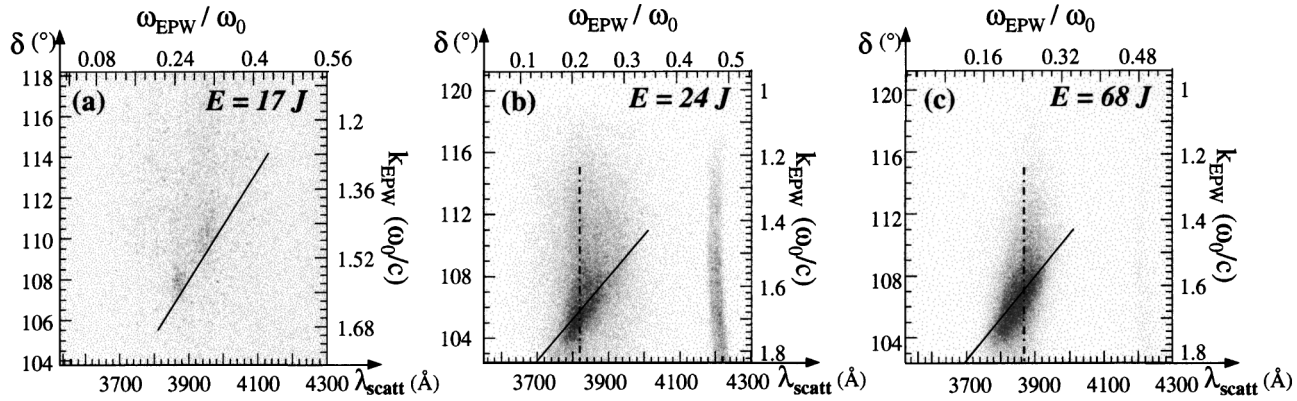

FIG. 2. Spectrum of the light Thomson scattered off EPWs for a laser energy equal to (a) 17 J, (b) 24 J, and (c) 68 J. The k_{EPW} and ω_{EPW} axes are shown in correspondence to the measured parameter δ and λ_{scatt} axes. For these shots, the collection volume was located in the front part of the plasma at 250 μm from the initial target plane where the maximum of Raman activity was observed. The spectral resolution is 40 Å.

energy case. The scattered intensity at $n_e/n_c = 0.076$ and its decomposition into EPW peaks are plotted in Fig. 3b as a function of the EPW wave vector. In this case, the spectrum is steeper than in the middle energy case: The relative line intensities of the components EPW1, EPW3, and EPW5 are 1:0.33:0.1. The total energy transferred in the cascade EPWs in that case is found to be less than the energy of the primary EPW. We therefore conclude that in the high laser energy case a smaller part of the SRS energy is transferred into the cascade decay products than in the medium energy case.

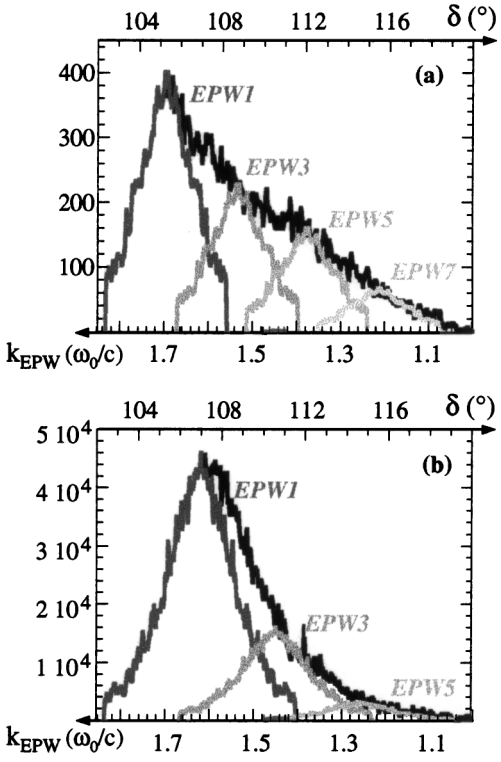

FIG. 3. (a) Scattered intensity (in arbitrary units) and its decomposition into the EPW1, EPW3, EPW5, and EPW7 contributions at $n_e/n_c = 0.055$ as a function of the probed EPW wave vector for a laser energy of 24 J. The corresponding section is shown by the dotted vertical line in Fig. 2b. (b) The same plot as in panel (a) but for the spectrum measured at 68 J at $n_e/n_c = 0.076$. The units are the same in both panels so that the respective level for these two plots can be compared.

We now show that the broadening of the IAW Thomson scattering spectra is in agreement with the number of LDI cascades deduced from the EPW spectra. Figure 4 shows that the broadening of each IAW TS peak is of the order of ~1.5 Å. Various sources may contribute to the width of each peak. First, the collected light is coming from a certain volume of plasma. The variation of the electron density across this volume produces a variation of wave number corresponding to a wavelength broadening of ~0.13 Å. The variation of the expansion velocity produces a broadening of ~0.53 Å [9]. The broadening resulting from these two sources is larger than the spectral resolution, 0.3 Å, but cannot account for the observed-spectral width of 1.5 Å. On the other hand, this observed width can be explained by the fact that each peak is the superposition of light scattered off IAWs coming from four

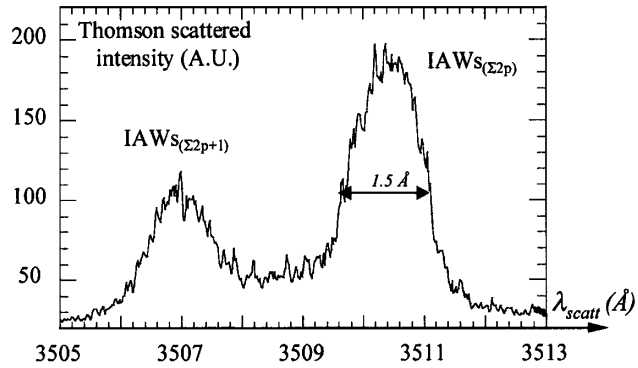

FIG. 4. Spectrum of down- and up-TS light off IAWs produced in the odd and even steps of the LDI cascade. This spectrum is time integrated over 100 ps around maximum scattered energy.

odd and even decays. Therefore, the IAWs spectra provide a complementary signature of the LDI cascade.

Though the two TS data clearly demonstrate the occurrence of the LDI cascade of the SRS generated EPW, the consequence of this cascade on SRS saturation is not immediately clear. The most important questions raised by our experimental results are the following: (i) Does the LDI cascade constitute a nonlinear saturation mechanism for SRS? (ii) Why does the width of the EPW k spectrum decrease with the intensity?

First, the LDI cascade does not give rise to saturation of the total SRS reflectivity in our experiment, because it is observed together with an exponential dependence of the SRS reflectivity on the laser energy [8]. This result is interpreted by the scenario [8,12] along which SRS essentially develops in those high intensity speckles whose power exceeds the critical power for self-focusing (SF). Indeed, the combination of a monotonous density profile with density modifications produced by speckle SF may give rise to local density minima, in which SRS becomes absolutely unstable. On the one hand, the LDI cascade may effectively saturate SRS in these speckles, as for a homogeneous plasma. On the other hand, the number of these self-focused speckles increases with the laser beam average intensity, resulting in an exponential dependence of the overall SRS reflectivity on the laser energy in the conditions of moderate laser energy corresponding to our experiments. In this scenario, the saturation of the SRS reflectivity could be observed for higher laser energy only, namely, in the regime where most of the speckles would satisfy the SF threshold.

Concerning question (ii), a possible explanation for the observed smaller number of cascades at higher laser intensity is the spatial scale shortening of the local density minima produced by the speckle SF. Indeed, the minimum EPW wave number that can be resolved in a density profile of the form $n_e(z) = n_0(1 + z^2/L_2^2)$ is $k_{\min} = (L_2\lambda_{De})^{-1/2}$, so that the maximum number of cascades is the ratio $k_{EPW1}/k_{\min}$. In the case of a medium laser intensity, L_2 is of the order of the Rayleigh length, $L_2 \sim 100\ \mu$m, with $\lambda_{De} \sim 0.01\ \mu$m, leading to a number of cascades of about 10, which is in qualitative agreement with Fig. 3a. In the high intensity case, speckle SF is more significant, leading to smaller L_2, which could be as small as 10 μm as seen in simulations [13]. Therefore, $k_{\min}$ increases approximately 3 times as compared with the medium laser intensity case, and the number of cascades decreases by the same amount, as observed in Fig. 3b.

In conclusion, the TS measurements of the EPWs and IAWs, together with the decomposition of the EPW k spectrum into the sum of the LDI cascade peaks, demonstrate the occurrence of the LDI cascade of the SRS generated EPW. For our experimental conditions, the LDI cascade does not lead to a large energy transfer towards the secondary EPWs and does not entail overall SRS saturation. This experimental result is interpreted as supporting the scenario [12] along which SRS activity essentially develops in the regime of absolute instability in the density dips generated by the self-focused speckles.

The authors gratefully acknowledge the support of A. Michard and of the technical groups of LULI. Part of this work was performed under the auspices of the U.S. Department of Energy by University of California Lawrence Livermore National Laboratory, through the Institute for Laser Science and Applications, under Contract No. W-7405-Eng-48.

*Present address: CEA/DIF, BP 12, 91680 Bruyères-le-Châtel, France.

[1] M. André, *Inertial Fusion Science and Applications* (Elsevier Gauthier Villars, Paris, 2000), p. 32.
[2] T. Dittrich *et al.,* Phys. Plasmas **6**, 2164 (1999).
[3] R. Kirkwood *et al.,* Phys. Rev. Lett. **77**, 2706 (1996); S. H. Glenzer *et al.,* Phys. Rev. Lett. **86**, 2565 (2001).
[4] S. H. Glenzer *et al.,* Phys. Rev. Lett. **80**, 2845 (1998); J. Lindl, Phys. Plasmas **2**, 3933 (1995).
[5] S. J. Karttunen, Phys. Rev. A **23**, 2006 (1981); J. A. Heikkinen and S. J. Karttunen, Phys. Fluids **29**, 1291 (1986).
[6] G. Bonnaud, D. Pesme, and R. Pellat, Phys. Fluids B **2**, 1618 (1990); B. Bezzerides, D. F. DuBois, and H. A. Rose, Phys. Rev. Lett. **70**, 2569 (1993); T. Kolber, W. Rozmus, and V. T. Tikhonchuk, Phys. Fluids B **5**, 138 (1993); D. F. DuBois, H. A. Rose, and D. A. Russell, Phys. Sci. **T63**, 16 (1996); R. L. Berger *et al.,* Phys. Plasmas **5**, 4337 (1998).
[7] D. A. Russell, D. F. DuBois, and H. A. Rose, Phys. Plasmas **6**, 1294 (1999).
[8] S. Depierreux *et al.,* Phys. Rev. Lett. **84**, 2869 (2000).
[9] S. Depierreux, C. Labaune, J. Fuchs, and H. A. Baldis, Rev. Sci. Instrum. **71**, 3391 (2000).
[10] Y. Kato *et al.,* Phys. Rev. Lett. **53**, 1057 (1984); J. Garnier, Phys. Plasmas **6**, 1601 (1999).
[11] D. M. Villeneuve, H. A. Baldis, J. E. Bernard, and R. Benesch, J. Opt. Soc. Am. B **8**, 895 (1991); D. M. Villeneuve *et al.,* Phys. Rev. Lett. **71**, 368 (1993).
[12] J. Fuchs *et al.,* Phys. Plasmas **7**, 4659 (2000); V. T. Tikhonchuk *et al.,* Phys. Plasmas **8**, 1636 (2001).
[13] A. Maximov *et al.,* Phys. Plasmas **8**, 1319 (2001).